



SAPIENZA
UNIVERSITÀ DI ROMA

**DEVELOPMENT AND INTEGRATION OF A SUBGRID
URBAN SURFACE SCHEME OVER A WIDE
METROPOLITAN AREA IN A LIMITED AREA MODEL**

ANTONIO CANTELLI¹, PAOLO MONTI², GIOVANNI LEUZZI²

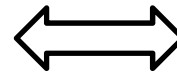
¹Department of Mechanical and Aerospace Engineering

²Department of Civil and Environmental Engineering



- Analysis of the impact of the inhomogeneities of the urban texture in the surface energy balance of a large city.
- The original surface scheme **LEAF3** integrated in RAMS is replaced by the **STEB** (Sub-grid TEB), an extension of the Town Energy Balance scheme (**TEB**, V. Masson, 2000, *BLM 94*), able to parameterize town-atmosphere dynamic and thermodynamic interactions.

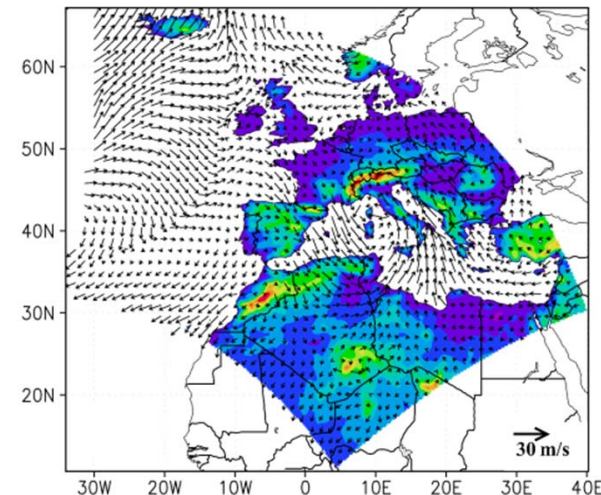
Urban canyon



Mesoscale model

Mechanical effects

Thermal effects



- Two subgrid schemes **STEB** of different complexities are developed, and the effects of the various simplifying hypothesis on the energy balance are investigated.

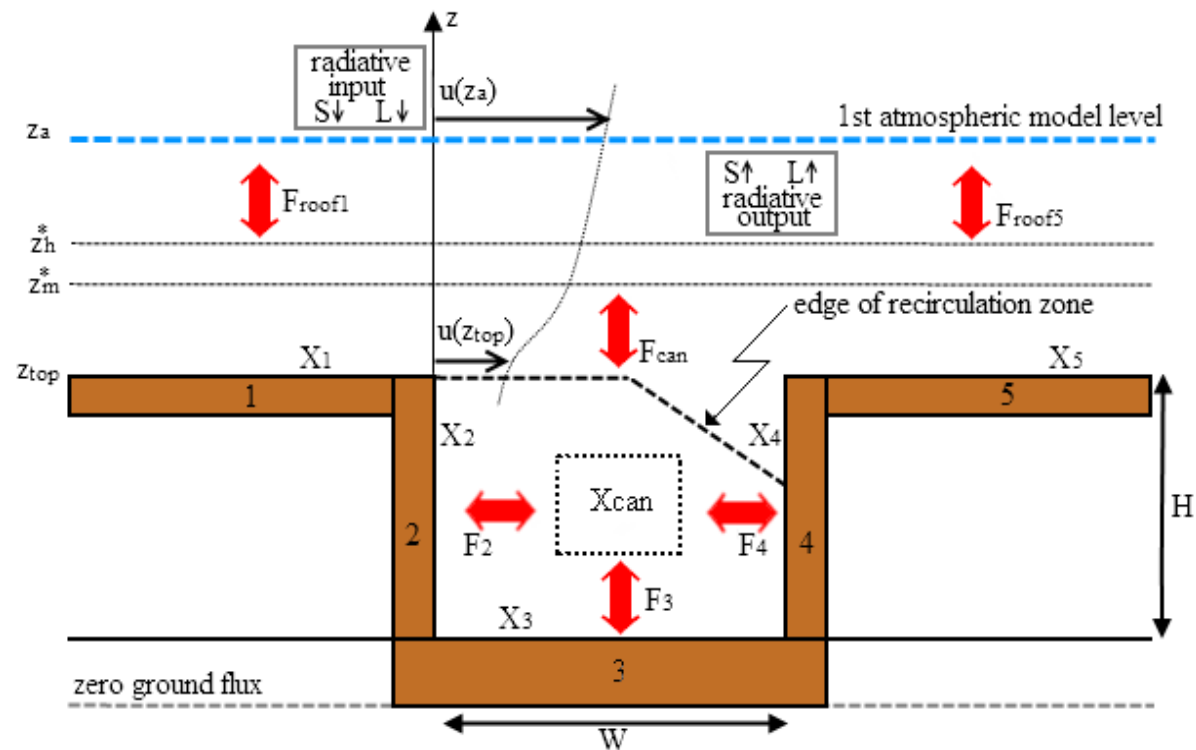


TEB (Town Energy Budget)

- **TEB** (Masson, 2000) calculates the turbulent fluxes exchanged by the canyon (1 wall, 1 road and the roof) with the atmospheric model.

$$Q^* + Q_F = Q_H + Q_E + G^* + \Delta Q_A \quad [\text{W m}^{-2}]$$

$$Q^* = S \downarrow - S \uparrow + L \downarrow - L \uparrow = Q_H + G^*$$

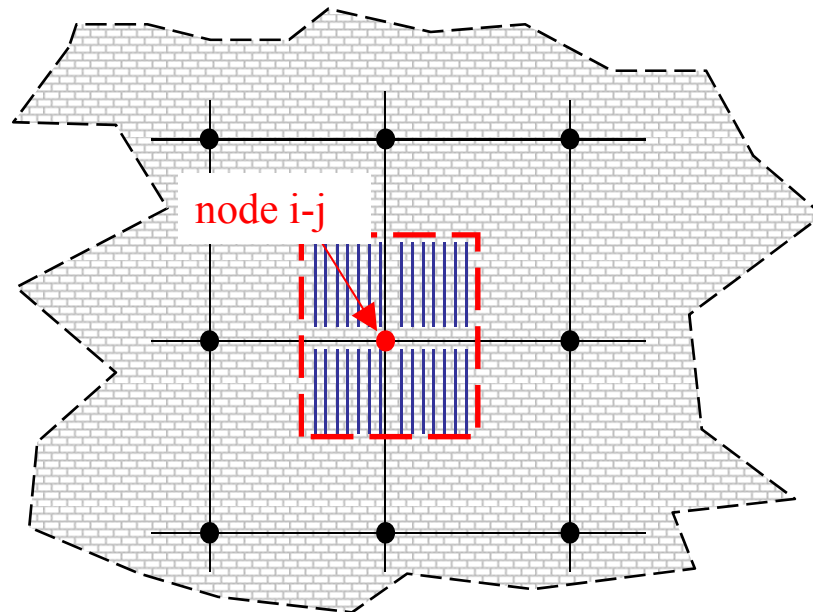




- It is based on the “canyon” assumption. From the energy balance (net solar radiation, sensible and latent heat fluxes, conduction heat fluxes) performed in each canyon, TEB calculates the temperatures of the three surfaces of the canyon:
 - ✓ Road
 - ✓ 1 vertical wall
 - ✓ Roof } **Three-facet scheme**
- It takes into account:
 - ✓ Sky viewing
 - ✓ Direct and reflected solar radiation
 - ✓ Trapping of longwave radiation by the canyon surfaces
 - ✓ Wind inside the canyon
 - ✓
- Main parameters:
 - ✓ Geometric \Rightarrow fractional area occupied by artificial materials, building height, building aspect ratio, Canyon aspect ratio, roughness length.
 - ✓ Radiative \Rightarrow roofs, roads and walls albedos and emissivity.
 - ✓ Thermal \Rightarrow thickness, thermal conductivity and heat capacity of roofs, roads and walls.
- TEB evaluates turbulent fluxes emitted from roofs and canyons towards the first grid level of the atmospheric model.

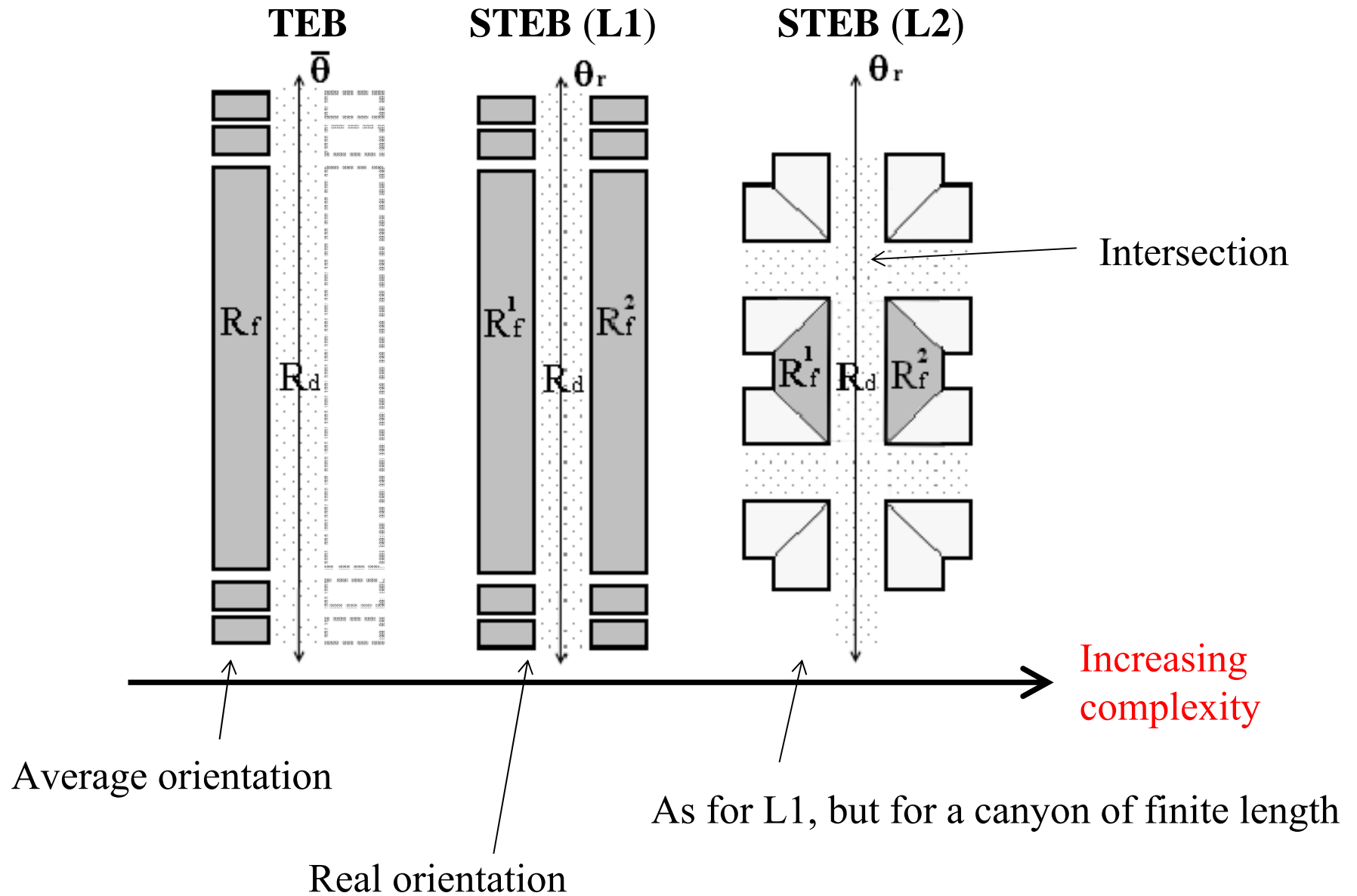


- The original **TEB** scheme is based on the following assumptions:
 - the canyons are equal among themselves,
 - they have infinite length,
 - they have not preferred orientation.





The Urban Canyon Schemes





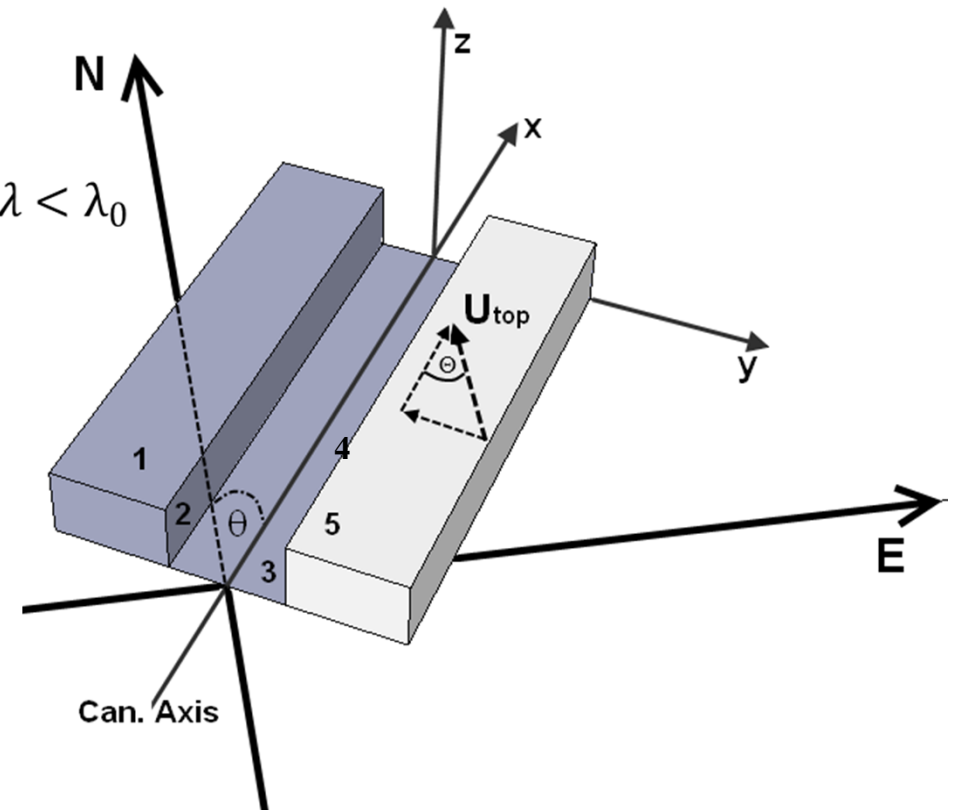
From L0 to L1

- **L1 is a four-facet scheme: 2 walls (2 & 4), 1 road (3) and the roof (1+5)**
- The equations for the solar radiations are rewritten to model the orientation:

$$S_{2,4-dir}(\theta) = \begin{cases} S_{dir} \tan\lambda |\sin\theta|, & \text{for } \lambda < \lambda_0 \\ S_{dir} \Downarrow \frac{W}{H}, & \text{for } \lambda \geq \lambda_0 \end{cases}$$

$$S_{3-dir}(\theta) = \begin{cases} S_{dir} \left(1 - \frac{H}{W}\right) |\sin\theta| \tan\lambda, & \text{for } \lambda < \lambda_0 \\ 0, & \text{for } \lambda \geq \lambda_0 \end{cases}$$

- λ is the zenithal angle
- $\lambda_0 = \arctan(W/H)$
- $W/H =$ canyon aspect ratio

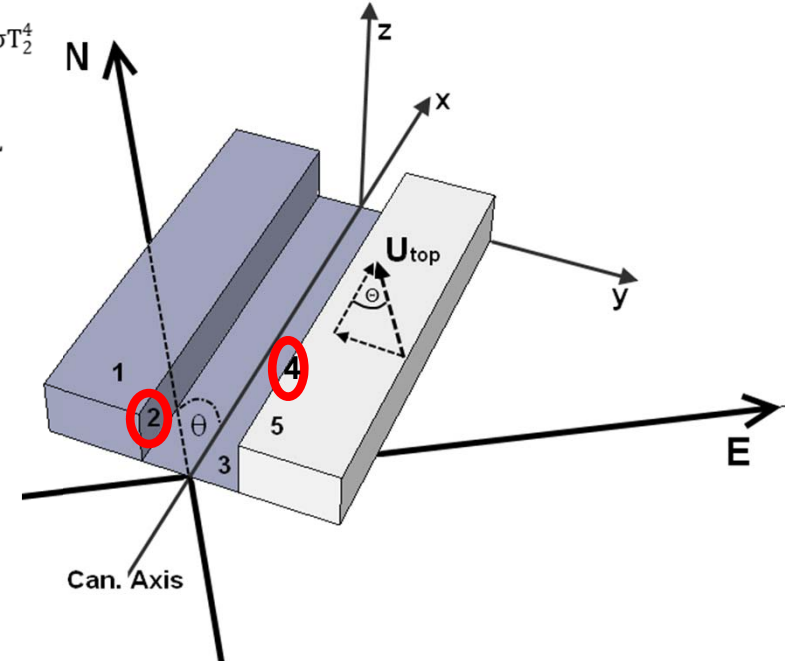




Infrared radiation

$$L_2^* = \psi_2 \varepsilon_2 \varepsilon_3 \sigma T_3^4 + (0.5 - \psi_2) \varepsilon_2 \varepsilon_4 \sigma T_4^4 + (0.5 - \psi_4) \varepsilon_2 \varepsilon_4 \sigma T_2^4 + \psi_2 \varepsilon_2 L - \varepsilon_2 \sigma T_2^4 \\ + \varepsilon_2 \sigma \psi_2 (1 - \varepsilon_3) (1 - \psi_3) \frac{1}{2} (\varepsilon_2 T_2^4 + \varepsilon_4 T_4^4) \\ + \varepsilon_2 \sigma (1 - 2\psi_2) (1 - \varepsilon_4) \left[(1 - 2\psi_4) \varepsilon_2 T_2^4 + \psi_4 \varepsilon_3 T_3^4 \right] + \varepsilon_2 L \\ \downarrow \left[\psi_3 \psi_2 (1 - \varepsilon_3) + \psi_4 (1 - 2\psi_2) (1 - \varepsilon_4) \right]$$

$$L_4^* = \psi_4 \varepsilon_4 \varepsilon_3 \sigma T_3^4 + (0.5 - \psi_4) \varepsilon_2 \varepsilon_4 \sigma T_2^4 + (0.5 - \psi_2) \varepsilon_2 \varepsilon_4 \sigma T_4^4 + \psi_4 \varepsilon_4 L \\ \downarrow - \varepsilon_4 \sigma T_4^4 + \varepsilon_4 \sigma \psi_4 (1 - \varepsilon_3) (1 - \psi_3) \frac{1}{2} (\varepsilon_2 T_2^4 + \varepsilon_4 T_4^4) \\ + \varepsilon_4 \sigma (1 - 2\psi_4) (1 - \varepsilon_2) \left[(1 - 2\psi_2) \varepsilon_4 T_4^4 + \psi_2 \varepsilon_3 T_3^4 \right] + \varepsilon_4 L \\ \downarrow \left[\psi_3 \psi_4 (1 - \varepsilon_3) + \psi_2 (1 - 2\psi_4) (1 - \varepsilon_2) \right]$$



$$S_2^* = (1 - \alpha_2) (S_{2-dir} + S_{2-dif}) + (1 - \alpha_2) (1 - 2\psi_2) M_4 + (1 - \alpha_2) (\psi_2) M_3$$

$$S_3^* = (1 - \alpha_3) (S_{3-dir} + S_{3-dif}) + (1 - \alpha_3) (1 - \psi_3) (M_2 + M_4) 0.5$$

$$S_4^* = (1 - \alpha_4) (S_{4-dir} + S_{4-dif}) + (1 - \alpha_4) (1 - 2\psi_4) M_2 + (1 - \alpha_4) (\psi_4) M_3$$

$$S_{1,5}^* = (1 - \alpha_{1,5}) (S_{1,5-dir} + S_{1,5-dif})$$

Solar
radiation

Two distinct walls involve two prognostic equations for the temperature T



- Wind velocity, temperature and aerodynamic resistances in the roughness sublayer and within the canyon used in L1 are based on the works of:
 - De Ridder (2010). *Bound-Layer Meteorol* **134**.
 - Dyer (1974). *Bound-Layer Meteorol* **7**.
 - Garratt (1994). Cambridge University Press, Cambridge.
 - Harman, Barlow and Belcher (2004). *Bound-Lay Meteorol* **113**.
 - Kastner-Klein and Rotach (2004). *Bound-Layer Meteorol* **111**.
 - Mölder, Grelle, Lindroth and Halldin (1999). *Agricult Forest Meteorol* **98**.
 - Soulhac, Perkins and Salizzoni (2008). *Bound-Layer Meteorol* **126**.
 - Yang, Tamai, Koike (2001). *J Appl Meteorol* **40**.



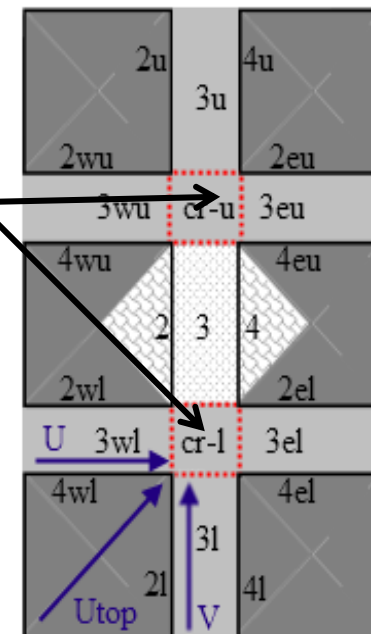
From L1 to L2

- In **L2** the canyon has a **finite length** → **intersections** are also considered
- No more canyons but buildings!!
- Sky view factors, solar and infrared radiations change accordingly.

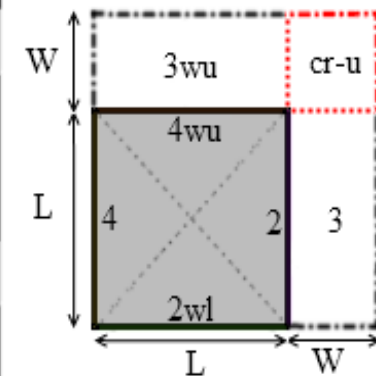
- Array of buildings
- Road intersections
- The energetic balance is rewritten to model all the surfaces which belong to each road

Note: 37 additional prognostic equations are needed for the temperature

Planar view



(a)

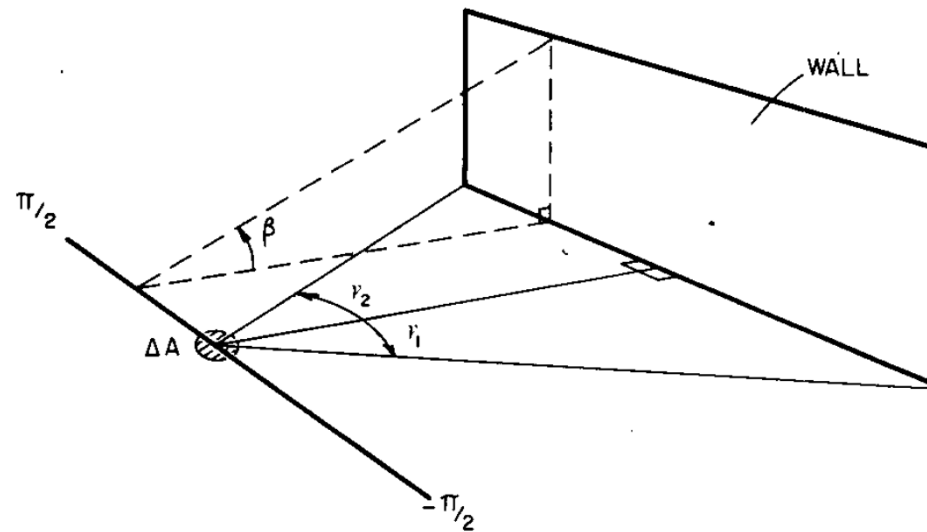


(b)



- The equations of the sky view factors are derived for a canyon of finite length (Johnson & Watson, 1981)

$$\psi_{w,w} = \frac{1}{2\pi} \int_A [\sin \gamma_2 \tan^{-1}(\tan \delta_2 \sin \gamma_2) + \sin \beta \tan^{-1}(\cot \delta_2 \sin \beta) + \sin \gamma_1 \tan^{-1}(\tan \delta_1 \sin \gamma_1) + \sin \beta \tan^{-1}(\cot \delta_2 \sin \beta)] dA$$



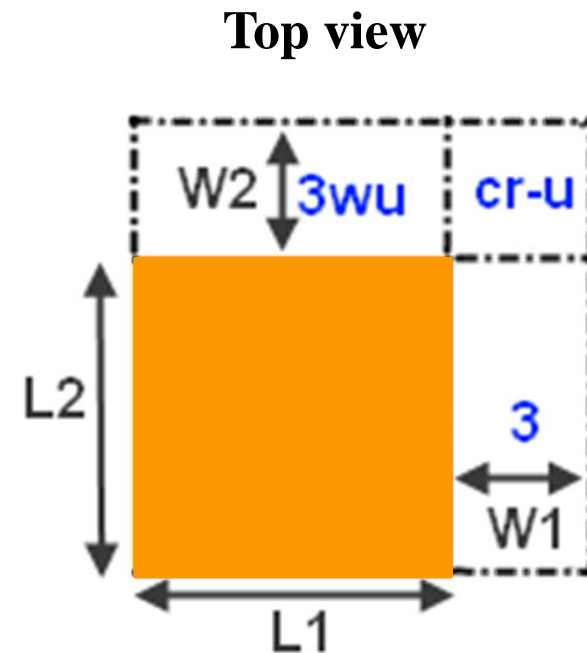


To simplify the model, the following assumptions can be introduced:

1. Buildings belonging to each canyon have the same height.
2. Materials with the same radiative and thermal properties.

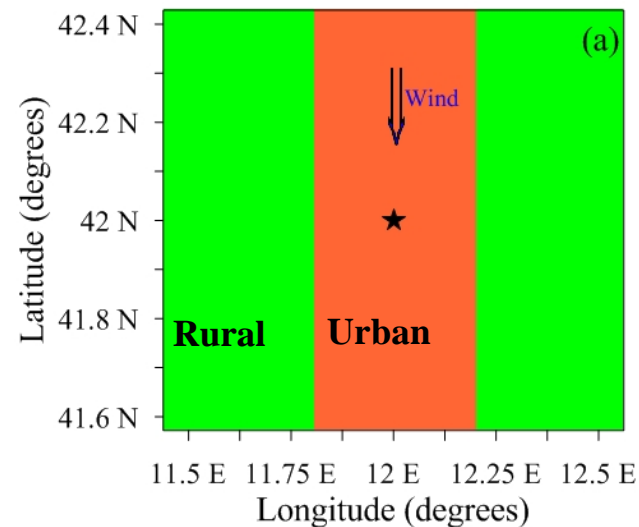


- Only one building of the array is considered in the numerical scheme.
- The prognostic equations involved in the scheme are 9 instead of 37.



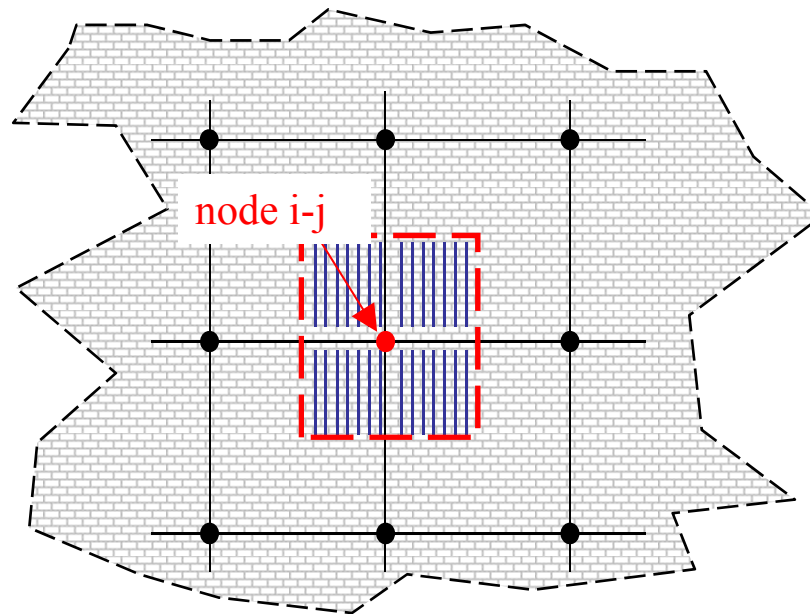


- The three schemes L0, L1 and L2 are integrated in RAMS 6.0.
- Numerical set-up:
 - Flat terrain (95x95 km²) in order to avoid any effect associated to the topography. Domain height: 21 km. 44 vertical grid nodes. Horizontal grid spacing: 1 km.
 - Summer and Winter conditions (15th of July; 21st of December) typical of the roman area (42°N).
 - All the urban cells have the same canyon geometry and the geostrophic wind is taken parallel to the urban fetch. No latent heat fluxes.





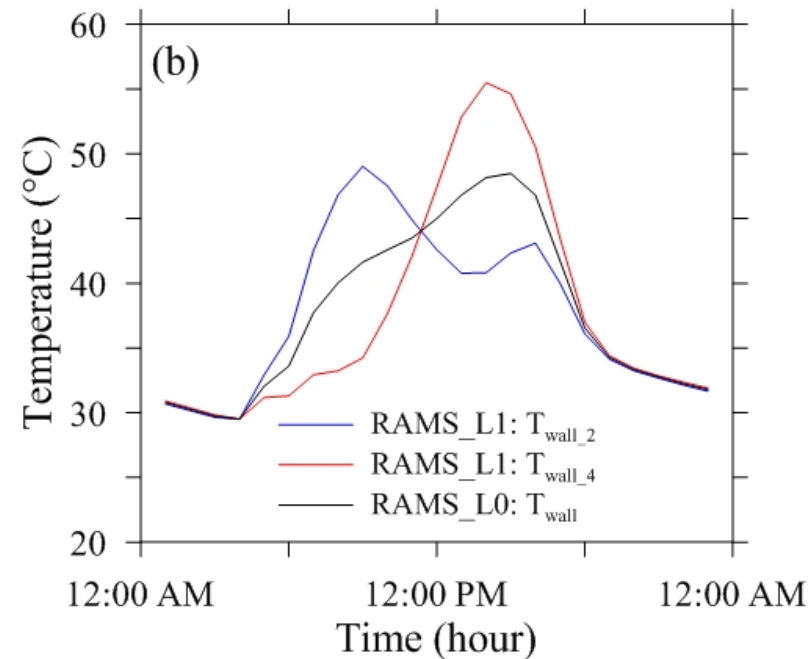
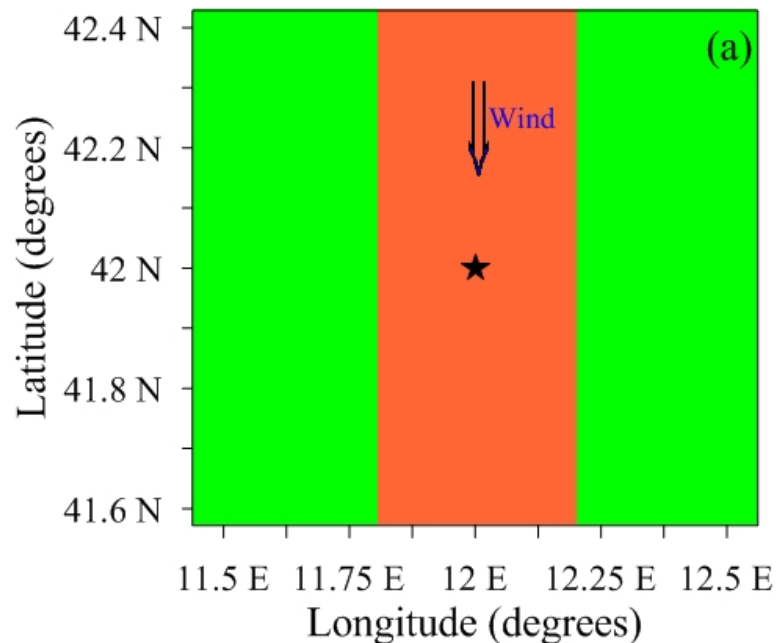
- Three simulations for each season are conducted with RAMS-L0 for $H/W=0.5$, 1 and 1.5.
- For RAMS-L1 and RAMS-L2, four runs for each aspect ratio are performed by varying the canyon orientation. Angles of 0° , 45° , 90° and 135° measured clockwise from North are considered for the analysis. The calculated variables are averaged over the four orientations.
- Building height $H=20$ m and plan areal fraction $\lambda_p=0.5$ equal for all the cases.
- Three days of simulation.





- For a single canyon orientation, L1 distributes the incident solar energy on both the canyon walls, and calculates the shadowing more precisely than L0.
- On average, L1 and L0 give the same results (as expected).
- Therefore, in the case of cities with preferred orientation of the canyons, the differences between L0 and L1 have to be taken into consideration to interpret the results.

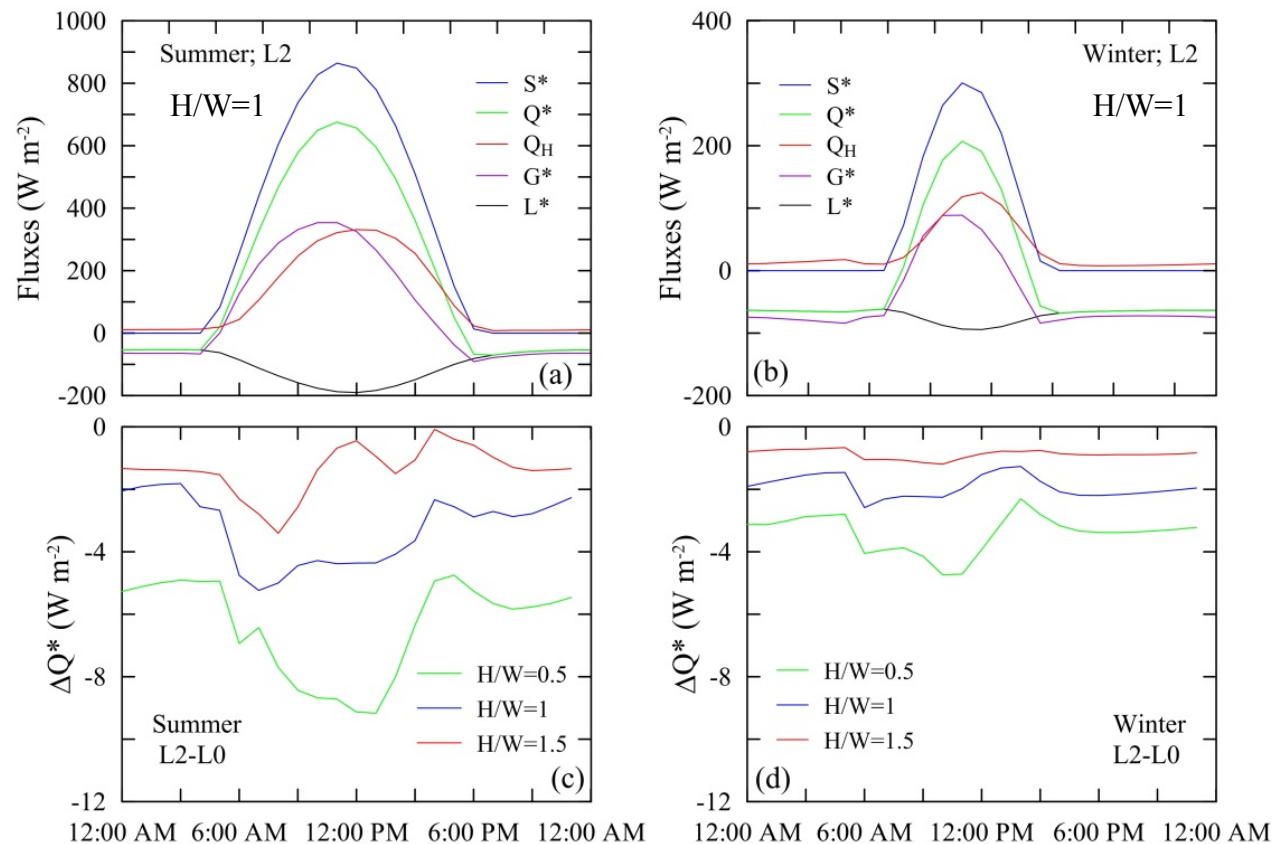
L0 (no orientation) vs. L1 (orientated canyons) : WALLS TEMPERATURE





Results (L2 vs. L0)

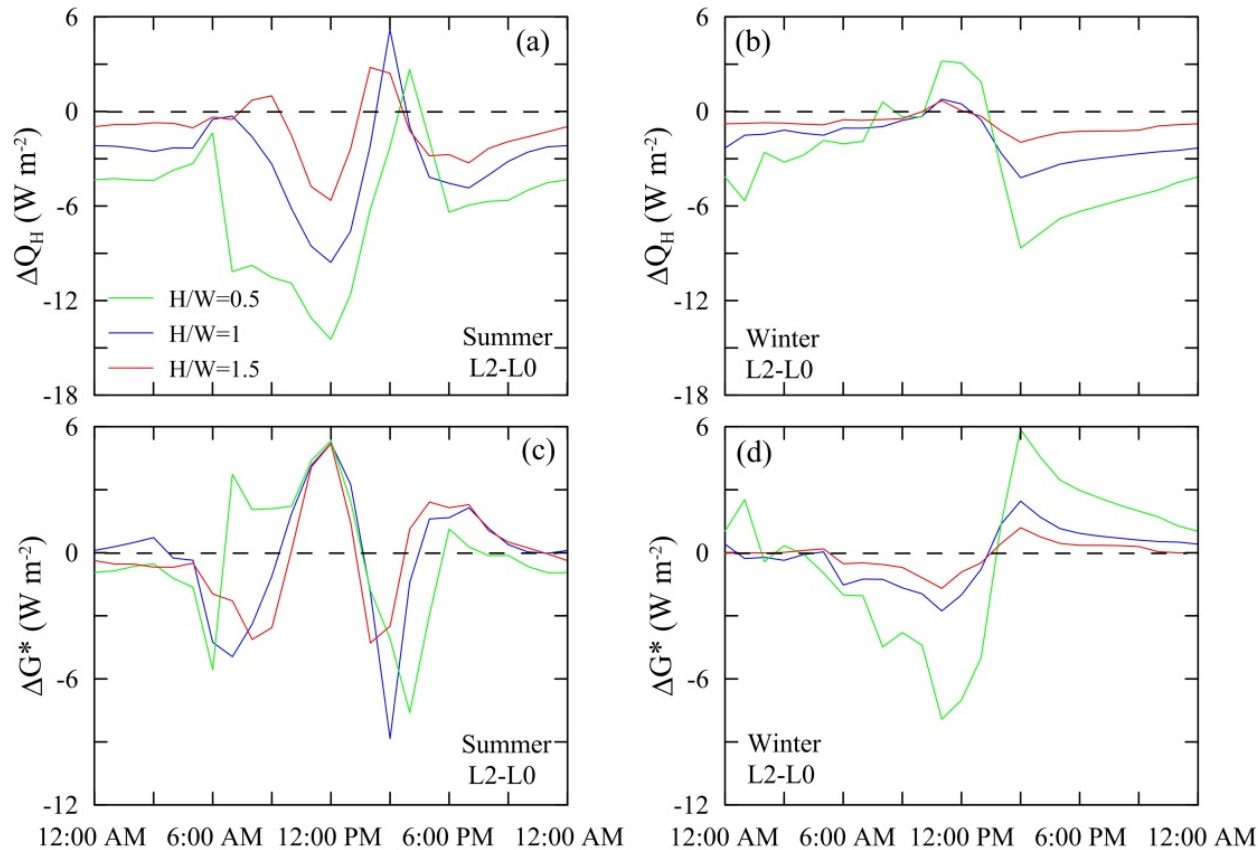
- The sensible heat flux Q_H remains positive all day long.
- The heat storage G^* reaches a positive maximum near 10 AM comparable with that attained by Q_H and becomes negative in the early afternoon.
- In winter G^* is negative for a large part of the day and reaches negative values of order -100 W m^{-2} .
- ΔQ^* for L2-L0 are associated to the different shadowing and sky view factors.





Results

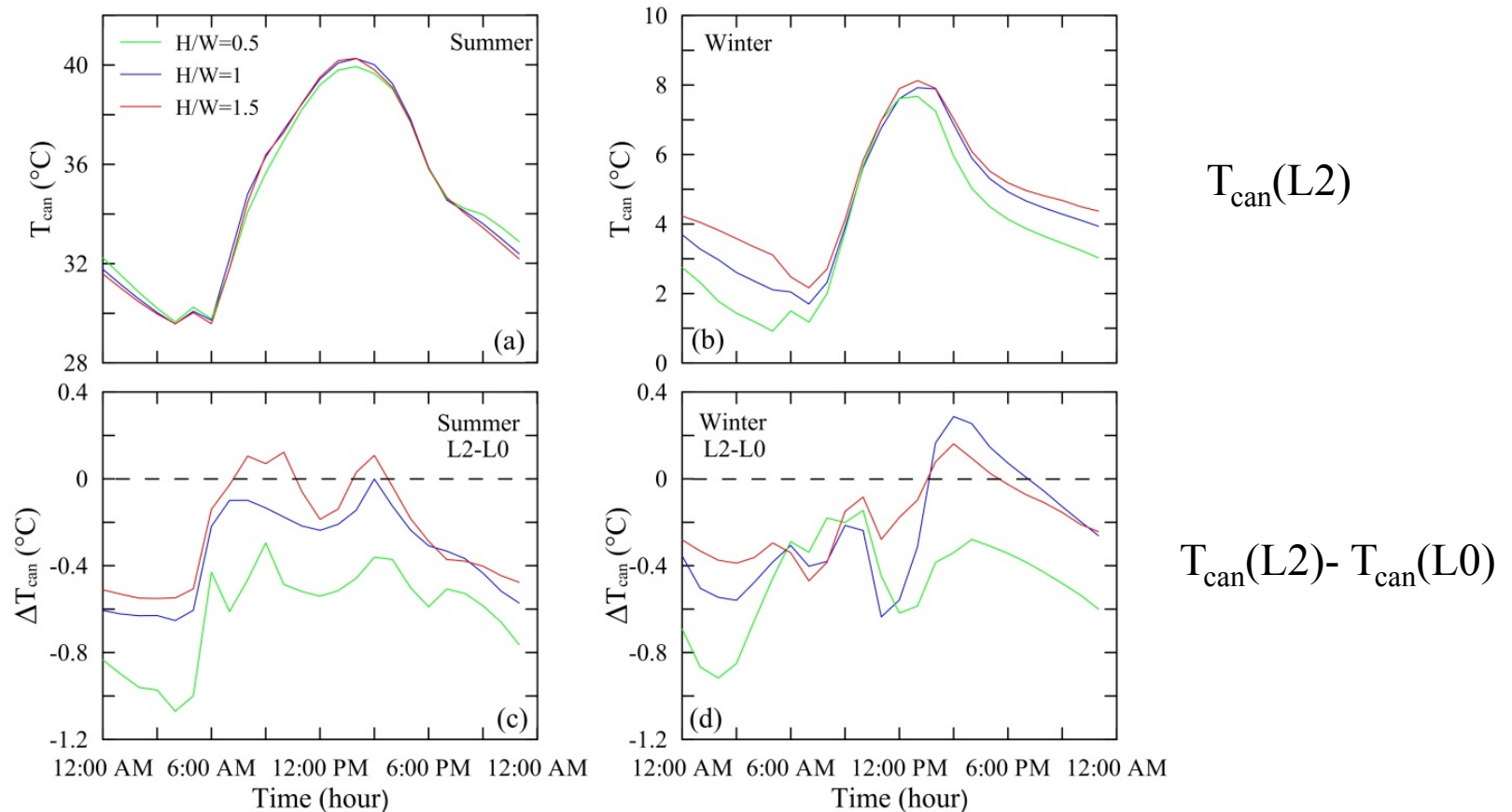
- L2 simulates generally lower Q_H than L0 during the day, particularly for $H/W=0.5$. In winter, ΔQ_H for the three H/W are less evident.
- G^* calculated by L2 is on average slightly lower than that calculated with L0 as a consequence of the larger sky view factors that increase the infrared radiation outgoing. As for the other energy fluxes, the higher ΔG^* occurs for $H/W=0.5$.





Results

- In winter the radiative trapping and the SVF are more important. T_{can} ($H/W=0.5$) is lower. In contrast, in summer there is an opposite behavior as a result of the importance of the effect of shadowing.
- In summer the larger ΔT_{can} occurs at night. These differences are significantly lower during the day.
- The differences occurring between the canyon schemes are associated mainly to the different SVF. There is (especially at night) a greater cooling of roads and walls. Since the differences between the SVF referred to L0 and L2 decreases as H/W increases, a canyon with aspect ratio $H/W=1.5$ modeled by L2 behaves similarly to L0.

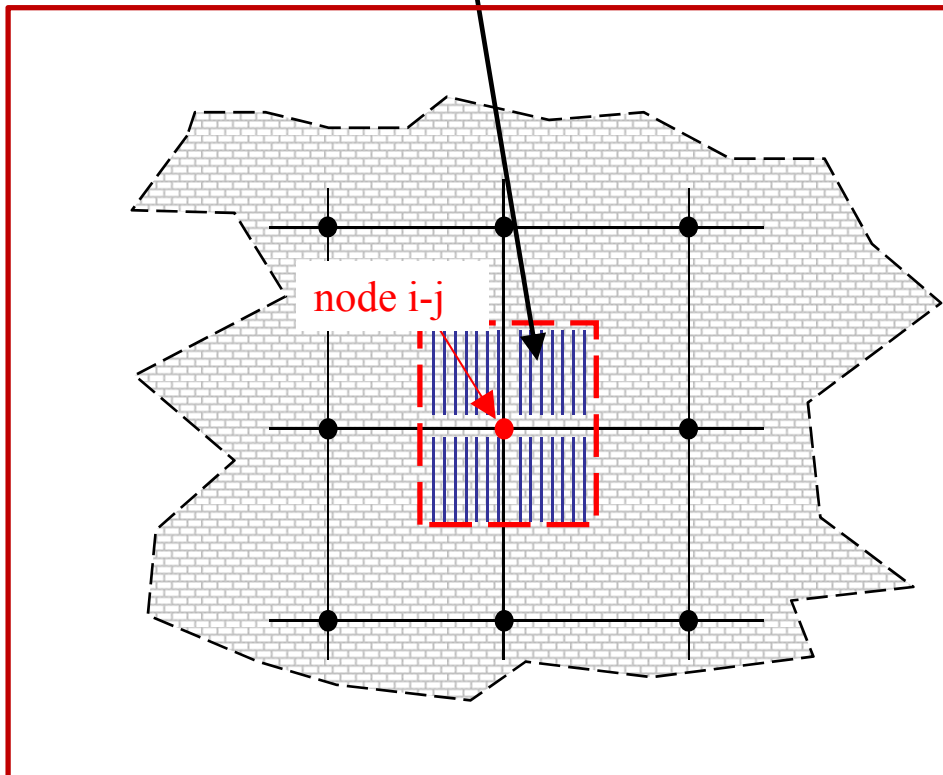




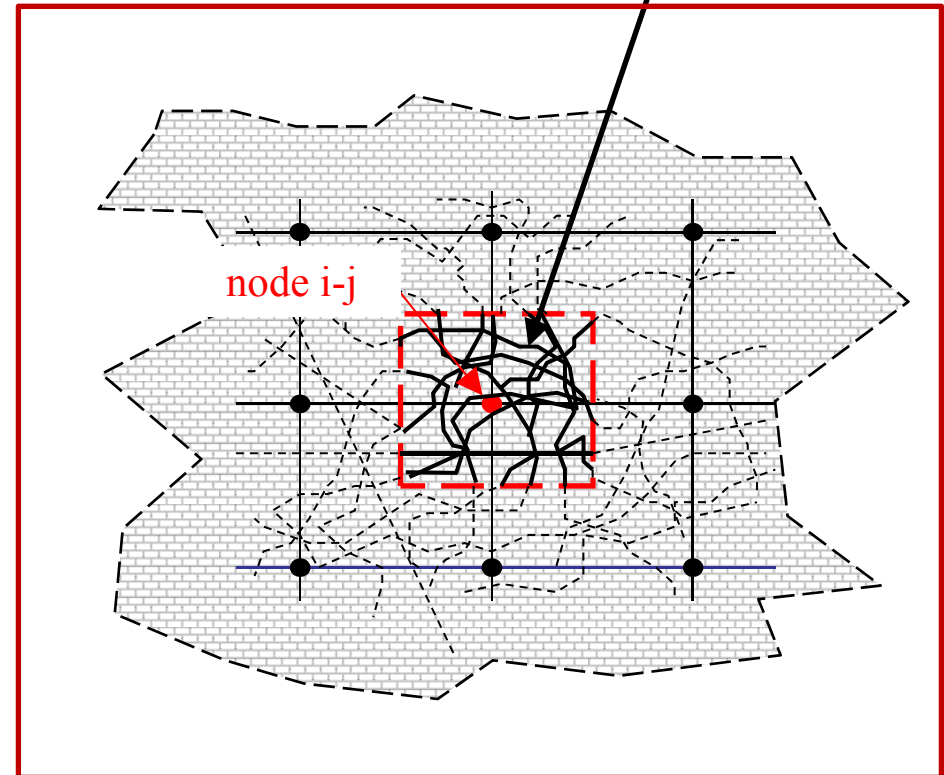
Application to a real case

- Generally, the TEB (L0) is integrated with a Mesoscale model by means of a “synthetic” town representation which considers an “average canyon”.
- In contrast, for a “true” town representation all the canyons belonging to the area of the grid are considered.

Texture of identical canyons



Texture composed of the actual canyons

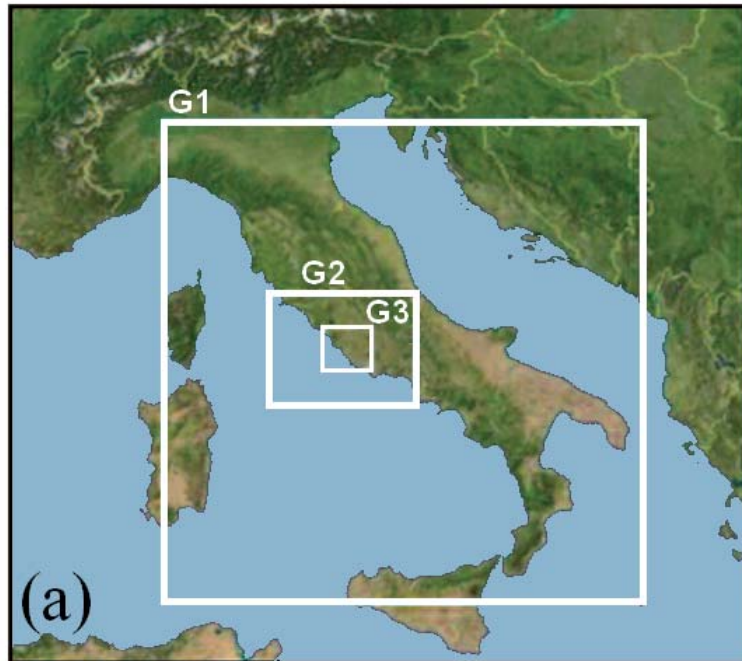




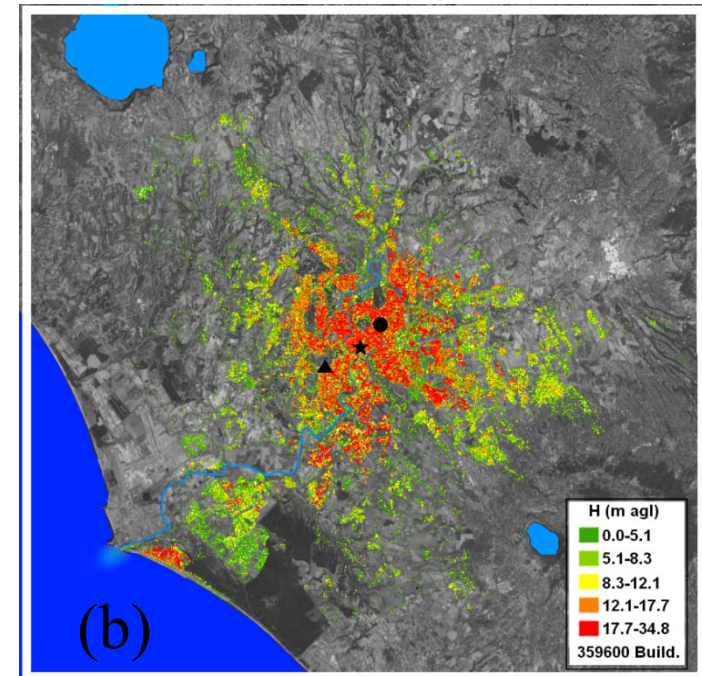
Application to a real case

- The true town representation is applied in a real case (Rome, Italy). Three nested grids are used, the finest one (G3) is 1 Km x 1 Km.
- 52 stretched sigma levels are used, with the lowest level at 11 m above the ground (for the grid G3). The model domain top is at 19 km.
- Analyzed period: 26-29 July 2005 (high pressure, light winds, ...)

Analyzed domain – 3 Grids



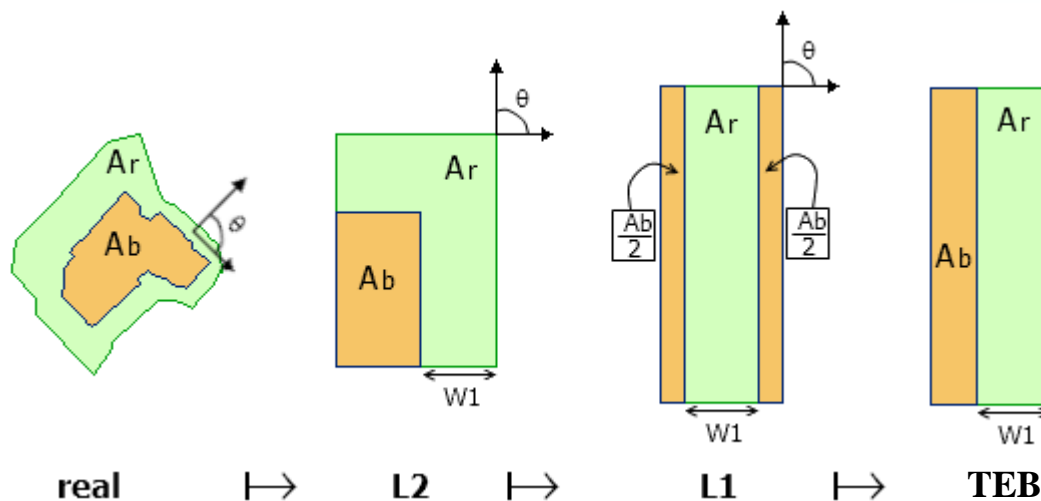
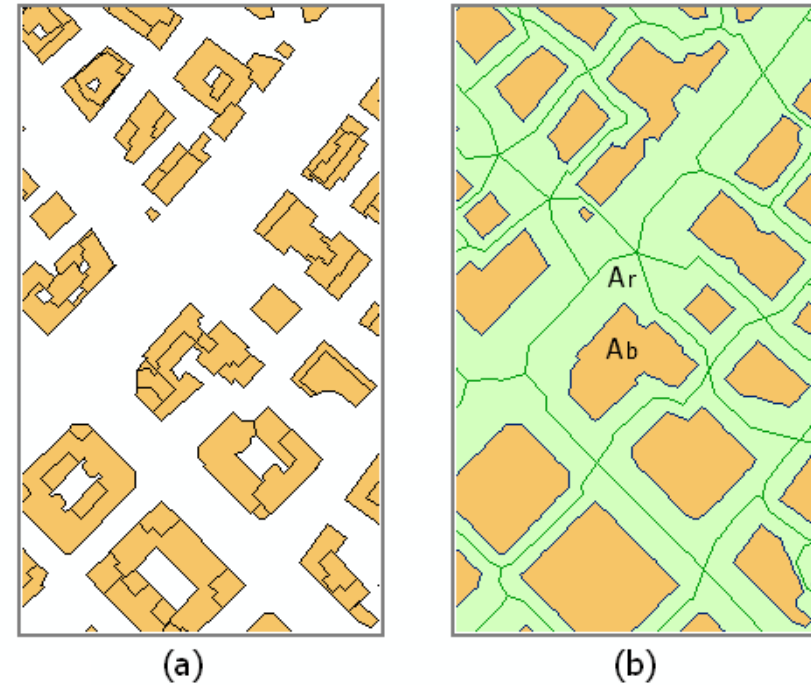
Grid G3: nearly 350,000 buildings





Application to a real case

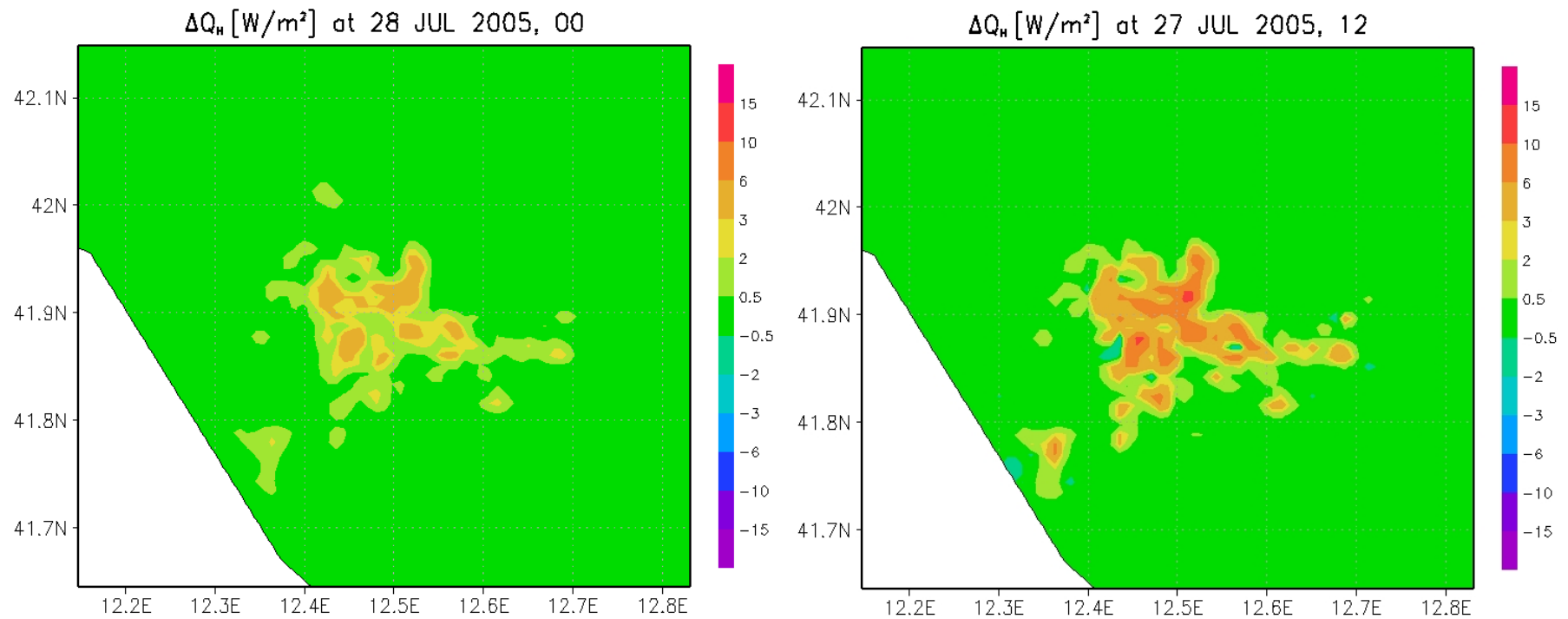
- High resolution urban DEM (a).
- Recognition of the single buildings (b):
 - Roof top area (A_b)
 - Road area (A_r).
- Each building is transformed according to the **L2** scheme.
- Successive transformations are made according to **L1** and **TEB** schemes.



The transformations **L2** \rightarrow **L1** and **L1** \rightarrow **TEB** preserve area and orientation of the building

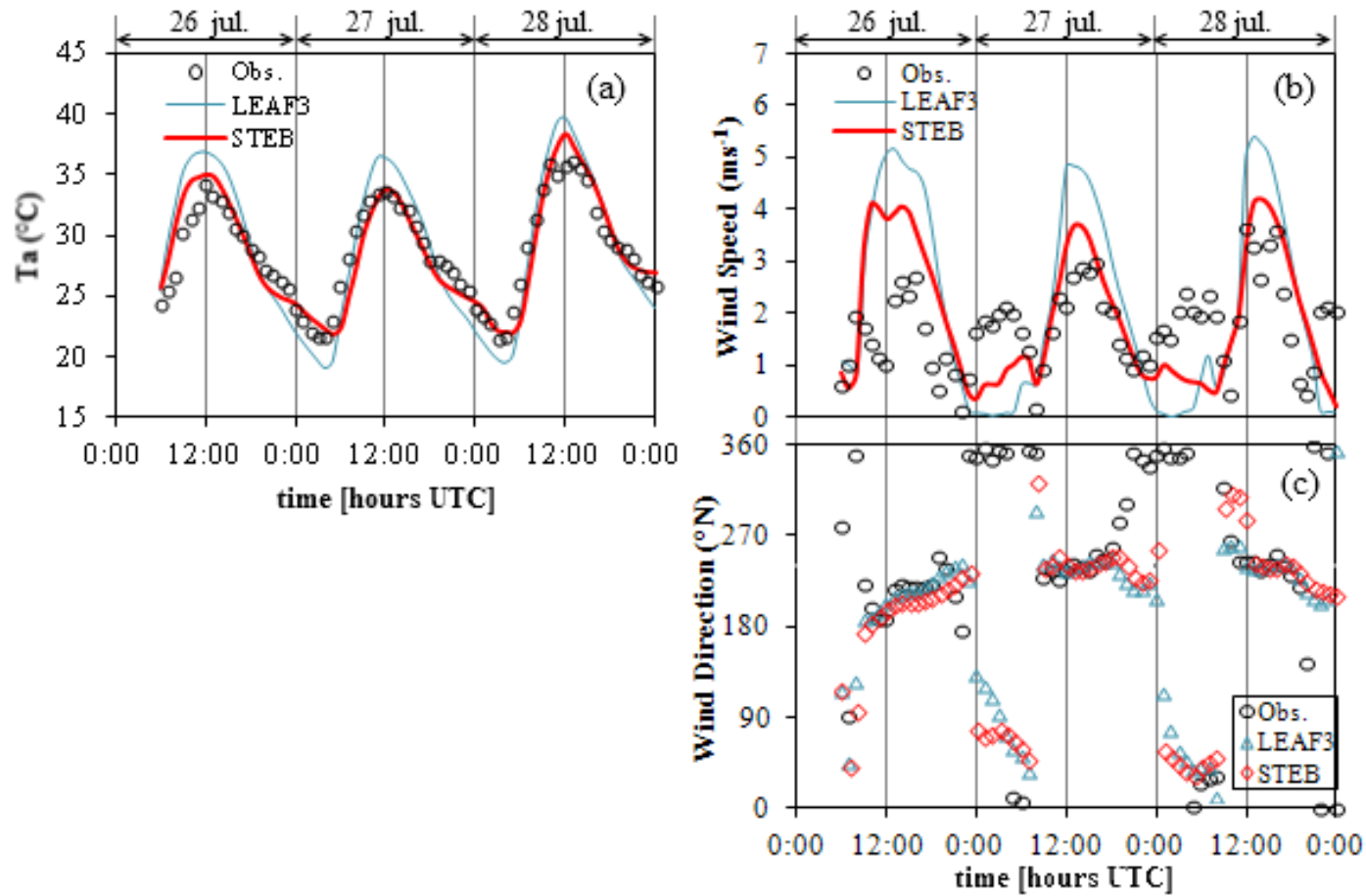


Differences between simulated Q_H (L0-L2)





Comparison between observations (Collegio Romano) and simulations (L2 and LEAF3)





- Starting from the canyon scheme TEB (Masson, 2000) two types of urban canyon models were developed, which include the canyon orientation and the presence of the intersections (canyons of finite length).
- L2 can be feed with urban DEM with high resolution and simulates the (approximated) presence of every single building.
- TEB overestimates the canyon temperature.
- L1 can be useful for urban complexes with preferred canyon orientation.
- The effect of the intersections (L2) is important in particular in summer for small H/W.
- L2 gives information on the wind velocity within the single canyon.
- Further investigation is needed to confirm the improvement of the results and the general applicability of the method.

Thanks for Your attention!!

$$\Psi_{3,i} = \frac{1}{2\pi} \int_A \{(\gamma_2 - \gamma_1) + \cos \beta [\tan^{-1}(\cos \beta \tan \gamma_1) - \tan^{-1}(\cos \beta \tan \gamma_2)]\} dA$$

$$\Psi_{i,j} = \frac{1}{2\pi} \int_A \left[\sin \gamma_2 \tan^{-1}(\tan \delta_2 \sin \gamma_2) + \sin \beta \tan^{-1}(\cot \delta_2 \sin \beta) + \right. \\ \left. + \sin \gamma_1 \tan^{-1}(\tan \delta_1 \sin \gamma_1) + \sin \beta \tan^{-1}(\cot \delta_1 \sin \beta) \right] dA$$

where $i,j=2,4$ with $i \neq j$.

$$\begin{cases} \Psi_2 = \Psi_{2,3} + 2(\Psi_{2,cr} + \Psi_{2,3eu^\infty} + \Psi_{2,3u^\infty}) \\ \Psi_3 = 1 - (2\Psi_{3,2} + 4\Psi_{3,2u^\infty} + 4\Psi_{3,2eu^\infty}) \\ \Psi_4 = \Psi_{4,3} + 2(\Psi_{4,cr} + \Psi_{4,3eu^\infty} + \Psi_{4,3u^\infty}) \end{cases}$$

$$L_2^* = \Psi_{3,2} \varepsilon_2 \varepsilon_3 \sigma T_3^4 + \Psi_{2,4} \varepsilon_2 \varepsilon_4 \sigma T_4^4 + \Psi_{4,2} \varepsilon_2 \varepsilon_4 \sigma T_2^4 + \Psi_2 \varepsilon_2 L \downarrow - \varepsilon_2 \sigma T_2^4 + \varepsilon_2 \sigma \Psi_{3,2} (1 - \varepsilon_3) 2\Psi_{3,2} \frac{1}{2} (\varepsilon_2 T_2^4 + \varepsilon_4 T_4^4) + \\ \varepsilon_2 \sigma 2\Psi_{2,4} (1 - \varepsilon_4) \left[2\Psi_{4,2} \varepsilon_2 T_2^4 + \Psi_{4,3} \varepsilon_3 T_3^4 \right] + \varepsilon_2 L \downarrow \left[\Psi_3 \Psi_{2,3} (1 - \varepsilon_3) + \Psi_4 2\Psi_{2,4} (1 - \varepsilon_4) \right] + L_2^{ed}$$

$$L_3^* = \Psi_{3,2} \varepsilon_3 \sigma [\varepsilon_4 T_4^4 + \varepsilon_2 T_2^4] + \Psi_3 \varepsilon_3 L \downarrow \\ - \varepsilon_3 \sigma T_3^4 + \varepsilon_3 \sigma (1 - \varepsilon_2) 2\Psi_{3,2} \frac{1}{2} \left[\Psi_{3,2} \varepsilon_3 T_3^4 + \Psi_{2,4} \varepsilon_4 T_4^4 \right] + \varepsilon_3 \sigma (1 - \varepsilon_4) 2\Psi_{3,2} \frac{1}{2} \left[\Psi_{4,3} \varepsilon_3 T_3^4 + \Psi_{4,2} \varepsilon_2 T_2^4 \right] + 2\Psi_{3,2} \varepsilon_3 L \downarrow \\ \frac{1}{2} \left[\Psi_2 (1 - \varepsilon_2) + \Psi_4 (1 - \varepsilon_4) \right] + L_3^{ed}$$

$$L_4^* = \Psi_{4,3} \varepsilon_4 \varepsilon_3 \sigma T_3^4 + \Psi_{4,2} \varepsilon_2 \varepsilon_4 \sigma T_2^4 + \Psi_{4,2} \varepsilon_2 \varepsilon_4 \sigma T_4^4 + \Psi_4 \varepsilon_4 L \downarrow \\ - \varepsilon_4 \sigma T_4^4 + \varepsilon_4 \sigma \Psi_{4,3} (1 - \varepsilon_3) 2\Psi_{3,2} \frac{1}{2} (\varepsilon_2 T_2^4 + \varepsilon_4 T_4^4) + \varepsilon_4 \sigma 2\Psi_{4,2} (1 - \varepsilon_2) \left[2\Psi_{2,4} \varepsilon_4 T_4^4 + \Psi_{2,3} \varepsilon_3 T_3^4 \right] + \varepsilon_4 L \downarrow \\ \left[\Psi_3 \Psi_{4,3} (1 - \varepsilon_3) + \Psi_2 2\Psi_{4,2} (1 - \varepsilon_2) \right] + L_4^{ed}$$

where L_2^{ed} , L_3^{ed} and L_4^{ed} are related to the infrared radiation coming beyond the edges of UC (from which the superscript "ed") from the surfaces located beyond the crossroads:

$$L_2^{ed} = 2\varepsilon_2 \varepsilon_2 \Psi_{2,2u} \sigma (T_4^4 + T_2^4) + 2\varepsilon_2 \varepsilon_2 \Psi_{2,2eu} \sigma (T_{2eu}^4 + T_{4eu}^4) + 2\varepsilon_2 \left[\varepsilon_3 \sigma (\Psi_{2,3u} T_{3u}^4 + \Psi_{cr,2} T_{cr}^4 + \Psi_{2,3eu} T_{3eu}^4) \right]$$

$$L_3^{ed} = 2\varepsilon_3 \varepsilon_2 \Psi_{3,2u} \sigma (T_4^4 + T_2^4) + 2\varepsilon_3 \varepsilon_2 \Psi_{3,2eu} \sigma (T_{2eu}^4 + T_{4eu}^4)$$

$$L_4^{ed} = L_2^{cr}$$

The comparability of the results obtained with the three UC schemes implies that the condition that all UCs have the same λ_p is attained. Since L2 has two mutually orthogonal UCs and one crossroad between them, it can be shown (Appendix C) that λ_p is maintained (assuming that the two UCs have the same length, H and H/W) if the UC length L is:

$$L = W \left(-1 + \frac{1}{\sqrt{\lambda_p}} \right)^{-1}$$

For example, for $\lambda_p=0.5$ and $H/W=0.5$ it results $L=96.6$ m. The condition of constant λ_p implies for L2 different lengths of roads as H/W changes. Since the view factors are heavily dependent on the wall length, by comparing the UCs with different lengths, a question arises on the comparability of the view factors for the three simulations. In order to ensure this, in L2 we maintain for $H/W=1$ and 1.5 the same canyon length as for $H/W=0.5$. At the same time, in the heat flow calculation attention is paid to consider the equivalent roof surface that would ensure the maintenance of $\lambda_p=0.5$.